JOURNAL OF CATALYSIS 148, 673–682 (1994)

# Strategies in Controlling the Homogeneity of Zirconia–Silica Aerogels: Effect of Preparation on Textural and Catalytic Properties

J. B. Miller, S. E. Rankin,[1] and E. I. Ko[2]

*Department of Chemical Engineering, Carnegie Mellon University, Pittsburgh, Pennsylvania 15213*

Received January 14, 1994; revised April 6, 1994

**We have used a sol–gel synthesis, followed by supercritical drying, to prepare zirconia–silica aerogels with different molecular ratios and varying degrees of homogeneity. Even at levels as low as 1–5 mol%, silica retards surface area loss and phase transformations that would normally occur in zirconia samples upon heat treatment. At 5 mol% silica, prehydrolysis of the silicon precursor tetraethylorthosilicate produces mixed oxide gels whose textural properties, most notably surface area and pore size distribution, vary with gel time in a manner that parallels pure zirconia aerogels. This evidence suggests that prehydrolysis effectively matches precursor reactivities and, in turn, produces homogeneous mixed oxides. Choosing an alternate silicon precursor, tetramethylorthosilicate, or chemically modifying the zirconium precursor by treatment with acetylacetone is also effective in matching precursor reactivity. Well-mixed 95 mol% zirconia–5 mol% silica aerogels are more active in 1-butene isomerization than are poorly mixed samples or either single component aerogel.**

## INTRODUCTION

Metal oxides have many applications in chemical and petrochemical processing as supports for catalytically active materials and as catalysts themselves. Mixed oxides, with two or more components, are also of significant scientific and commercial interest. Incorporation of a minor oxide component can enhance the thermal stability of a major component (1–4), allowing it to be used at higher operating temperatures. The combination of two oxides can also enhance their catalytic activities. Mixed oxides often display surface acid strengths that are significantly higher than those of either of the component oxides (1, 2, 4–6). Such materials, most notably silica–aluminas, have been employed as industrial solid acid catalysts. Models proposed by Tanabe (7) and Kung (8) attribute the generation of acidity in mixed oxide samples to charge imbalances that exist along $M$–O–$M'$ linkages, where $M$ and $M'$ represent two different cations. Therefore, we would expect samples in which component oxides are homogeneously distributed (i.e., well mixed) to exhibit favorable acidic properties. Indeed, both the relative amounts of the components in a mixed oxide and how well they are mixed have been observed to affect its textural, structural, and catalytic properties (2, 9–15).

Conventional mixed oxide preparation techniques do not usually produce molecularly homogeneous, high-surface-area materials. For example, the practice of calcining a mechanically ground mixture of component oxides or their solid-phase precursors can result in a well-mixed two-component oxide. However, the product is typically very dense, lacking the high surface area and pore volume usually desired for catalytic applications (16). Because hydroxides of different metallic cations generally do not precipitate at the same pH, molecular homogeneity is also difficult to achieve using the common coprecipitation technique (16, 17).

In contrast to these and other traditional preparation methods, the sol–gel synthesis of mixed oxide aerogels allows excellent control of mixing while stabilizing important textural characteristics, most notably high surface area and pore volume. Within the sol–gel process, relative precursor reactivity can be used to control homogeneity. In a qualitative manner, we expect the more reactive precursor to hydrolyze and condense first. The less reactive precursor hydrolyzes and condenses later, thereby coating or encapsulating the condensation products of the more reactive precursor to produce a segregated gel. On the other hand, when precursor reactivities are evenly matched we would expect a homogeneous gel to form.

Sol–gel chemistry offers four main strategies for controlling relative precursor reactivity. (i) For most metal atoms, more than one alkoxide precursor exists. Based on factors such as the inductive capability (which alters the electronegativity of the precursor's metal atom, a key

---

[1] Present address: Chemical Engineering and Materials Science Department, University of Minnesota, Minneapolis, MN 55455.

[2] To whom correspondence should be addressed.

0021-9517/94 $6.00

determinant of reactivity in nucleophilic substitution reactions) and steric hindrance of various alkoxy groups, we would expect different alkoxides of the same metal to display different reactivities (18). Therefore, simply choosing a different precursor molecule can often help match reactivities. (ii) An unreactive precursor can be given a head start by allowing it to "prereact" with water. This technique, known as prehydrolysis, is the most common reactivity matching scheme used in sol–gel syntheses (12, 14, 19–23). It is also the technique that we emphasize in this work. (iii) A reactive precursor can be slowed by replacing some of its alkoxy groups with different ligands in a technique known as "chemical modification" (24). Common modifiers are acetic acid and acetylacetone (25). Chemical modification has been used most often to control condensation rates in single oxide syntheses (24–28). (iv) When the precursors' reactivities respond to temperature differently, we might expect a change in the synthesis temperature to bring their reactivities closer together.

Even though each of these techniques has been demonstrated to be effective for controlling precursor reactivities in sol–gel systems, they have not yet been compared in a single study that emphasizes preparation of mixed oxides for catalytic applications. This work concerns the synthesis of 95 mol% zirconia–5 mol% silica aerogels using each of these precursor reactivity matching strategies. Our aim is to determine the effect of preparation on the textural and catalytic properties of the mixed oxide aerogels. Because homogeneity is difficult to define and measure at a molecular level, we infer the extent of mixing in our samples from their physical and catalytic properties.

Our interest in the zirconia–silica system follows from our work with pure zirconia (29), which itself has many significant catalytic applications (29–37). The zirconia–silica system has been investigated by other researchers (19–21, 38–42). However, in contrast to our work, many of these studies emphasize preparation of dense ceramics with low zirconia contents. As a catalyst, zirconia–silica has been reported to possess stronger acid sites than either silica or zirconia alone (5, 15). The introduction of small amounts of silica into zirconia has been observed to impart stability against surface area loss and crystallization upon heating (15). In this paper we report results of zirconia–silica aerogels that provide new insight into both of these important observations.

## METHODS

### *Synthesis of the Mixed Oxide Aerogels*

Table 1 lists the sol–gel parameters we used to prepare the gels studied in this work. For a typical nonprehydrolyzed (NPH) synthesis, nitric acid (Fisher, 70 wt%)

TABLE 1

Sol–Gel Parameters in Preparing the Alcogels

| Sample[a] | $HNO_3/Zr^{(4+)}$ (ml/mol) | $HNO_3/Si^{(4+)}$ (ml/mol) | $HNO_3/M^{(4+)}$ (ml/mol) | Preparation technique[b] | Gel time (s) |
|---|---|---|---|---|---|
| *Low-silica series* | | | | | |
| A-ZrO$_2$#73[c] | —[d] | — | 52 | — | 35 |
| A-PH-ZS99#3 | 52.8 | 6.3 | 52 | PH-TEOS | 26 |
| A-PH-ZS98#2 | 53.2 | 6.3 | 52 | PH-TEOS | 32 |
| A-PH-ZS95#19 | 47.0 | 6.3 | 45 | PH-TEOS | 33 |
| *Stair-step series* | | | | | |
| A-NPH-ZS95#10 | — | — | 40 | NPH-TEOS | 28 |
| A-PH-ZS95#53 | 52.3 | 6.3 | 50 | PH-TEOS | 49 |
| A-NPH-ZS95#27 | — | — | 45 | NPH-TEOS | 52 |
| A-PH-ZS95#49 | 57.6 | 6.3 | 55 | PH-TEOS | 114 |
| A-NPH-ZS95#25 | — | — | 50 | NPH-TEOS | 113 |
| *Alternate reactivity matching techniques* | | | | | |
| A-NPH-ZS95#29 | — | — | 50 | NPH-TMOS | 70 |
| A-NPH(AC)-ZS95#11 | — | — | 45 | NPH-TEOS-AC | 64 |
| A-PH-ZS95#59 | 54.3 | 6.3 | 52 | PH-TEOS | 67 |
| A-NPH(T)-ZS95#3 | — | — | 40 | NPH-TEOS | 137 |

[a] Notation: A, aerogel; PH, prehydrolyzed; NPH, nonprehydrolyzed; AC, acac-modified zirconium precursor; T, synthesis performed in ice bath; ZS*xx*, zirconia–silica mixed oxide with *xx* mol% zirconia; #yy, batch number.

[b] Held constant: 36 ml 1-propanol total solvent, $M^{(4+)}$/*1*-propanol = 1.0 mmol/ml and $H_2O/M^{(4+)}$ = 2.0 mol/mol.

[c] Pure zirconia aerogel; see Ref. 29.

[d] Not applicable to ZrO$_2$ and NPH samples because nitric acid was added to a single solution.

was added to 15 ml of 1-propanol (Fisher certified). Next, in a nitrogen-purged glove box, zirconium *n*-propoxide (Johnson–Matthey, 70 wt% in 1-propanol) and tetraethylorthosilicate (TEOS, Aldrich) were added. Finally, a second solution of water in 15 ml of 1-propanol was poured into the precursor solution. The mixture was agitated by a magnetic stir bar. We define gel time as the elapsed time between addition of the final solution and the point at which the stirrer can no longer produce a vortex in the reaction mixture.

In a typical prehydrolyzed (PH) synthesis, TEOS was mixed with 20 ml of 1-propanol in a glove box. Next, a portion of the hydrolysis water and a portion of the nitric acid were added to the TEOS solution, which was then covered and stirred for a 10-min prehydrolysis period. Upon completion of prehydrolysis, the remaining nitric acid was added and the solution returned to the glove box for addition of the zirconium precursor. Finally, a solution containing the remaining water in 10 ml 1-propanol was poured into the mixed precursor solution and the gel time measured as described above.

The gel made with an acetylacetone (acac)-modified zirconium precursor was prepared by first dissolving the acetylacetone (Fisher) in 8.5 ml of 1-propanol. In a glove box, the zirconium precursor was then added. The solution was covered and allowed to stir for 10 min. Next, a solution of nitric acid in 7 ml of 1-propanol was added, followed by the silicon precursor. The mixed precursor solution was removed from the glove box and combined with a solution of water in 14 ml of 1-propanol.

The TMOS gel was prepared using a tetramethylorthosilicate (Aldrich) silicon precursor. Its synthesis is otherwise the same as that of an NPH-TEOS gel. The low-temperature gel was made by combining the two final solutions of an NPH synthesis in an ice bath.

Each gel was covered with plastic film and allowed to age for 2 h at room temperature. The alcohol solvent was subsequently removed by contact with flowing supercritical (343 K, ~2.2 × $10^4$ kPa) carbon dioxide in a supercritical extraction screening system (Autoclave Engineers, Model 08U-06-60FS). At a $CO_2$ flow rate of ~1400 ccm (ambient conditions), the solvent was completely removed in approximately 2 h.

The product powder was ground to <100 mesh before heat treatment. The first treatment was vacuum drying at 383 K for 3 h. Except for the acac-modified gel, which underwent an additional vacuum treatment at 573 K to remove tightly bound residual organics, the 383 K treatment was followed by a series of calculations in flowing oxygen (400 ccm) performed in a tube furnace. The vacuum-dried powder was first calcined for 2 h at 773 K. Further calcinations at 1173 and 1373 K were performed on samples that had previously been heated to773 K.

### *Characterization of the Mixed Oxide Aerogels*

Pore size distributions, BET surface areas, and pore volumes were measured by nitrogen adsorption/desorption using an Autosorb-1 system (Quantachrome Corp.). Prior to analysis, samples were outgassed under vacuum for 3 h at room temperature (non-heat-treated-samples), 373 K (vacuum-dried samples), or 473 K (all calcined samples).

Crystalline structure was determined by X-ray diffraction (XRD) experiments performed on a Rigaku D/Max diffractometer using Cu $K_\alpha$ radiation. Selected samples were characterized by diffuse reflectance IR spectroscopy (DRIFT, Mattson Galaxy Series FTIR 5020; samples 2 wt% in KBr).

Selected samples were also tested for their catalytic activity in 1-butene isomerization. Approximately 200 mg of mixed oxide was used as catalyst in a fixed bed, downflow reactor. The sample was first dried in 50 sccm helium (Matheson HP) at 473 K. The temperature of the sample was reduced to 423 K and the feed changed to a mixture of 5 sccm 1-butene (Matheson, research grade) and 95 sccm helium. The products—*cis*- and *trans*-2-butene—were quantified by gas chromatography (Gow-Mac 550P with thermal conductivity detector; Supelco 23% SP1700 on 80/20 Chromosorb column).

## RESULTS AND DISCUSSION

### *Textural Properties of the Low Silica Content Gels (0–5 mol%)*

The dependence of surface area and pore volume upon silica content for gels in this composition range is shown in Fig. 1. Note that the addition of even small amounts of silica increases both pore volume and surface area, presumably by retarding the sintering process. Figure 2 compares relative surface area (area after heat treatment

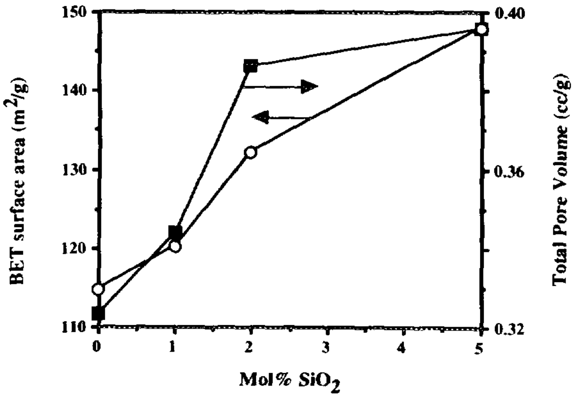

FIG. 1. BET surface area and pore volume as a function of silica content for low-silica zirconia–silica aerogels. All samples calcined at 773 K in oxygen for 2 h.

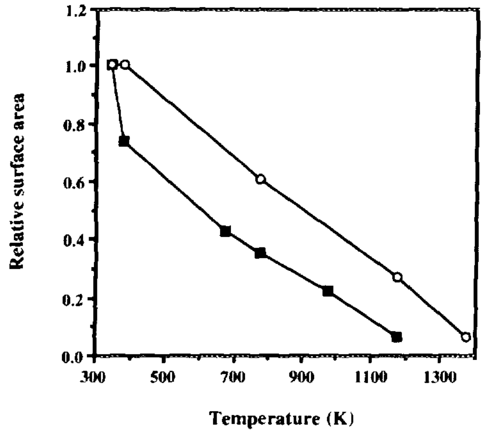

FIG. 2. Relative surface area (area after heat treatment at temperature $T$/area after supercritical drying) as a function of heat treatment temperature. Open symbols, A-PH-ZS95#19; closed symbols, A-$ZrO_2$#73.

at temperature $T$/area of supercritically dried sample) as a function of heat treatment temperature for samples containing 5 mol% silica and pure zirconia. At all temperatures, the mixed oxide retains a higher fraction of its original surface area than does the pure zirconia, clearly demonstrating silica's stabilizing effect. Figure 3 shows XRD patterns of the low-silica-content gels after calcination at 773, 1173, and 1373 K. As silica content is increased from 0 to 5 mol%, zirconia's transformations from X-ray amorphous to tetragonal and tetragonal to monoclinic are delayed to higher temperatures.

These behaviors are typical for the addition of small amount of dopants to zirconia (2, 15). We note that, in work reported by Soled and McVicker (15), 15 mol% silica is required to stabilize X-ray amorphous zirconia in a zirconia–silica xerogel (a sol–gel product dried by evaporation) calcined for 3 h at 773 K. With only 5 mol% silica, we stabilize X-ray amorphous zirconia in an aerogel calcined at 773 K for 2 h. Furthermore, at comparable compositions in the 0–5 mol% silica range, our mixed oxides have consistently higher surface areas (at 1 mol% silica, for example, 120 $m^2/g$ vs 48 $m^2/g$). Part of this difference is probably due to the shorter calcination time we use (2 h vs 3 h). However, some of the increased stability of our samples can be attributed to supercritical solvent removal. As we have described previously, supercritical drying yields an oxide network which is resistant to sintering and crystallization upon thermal treatment (43).

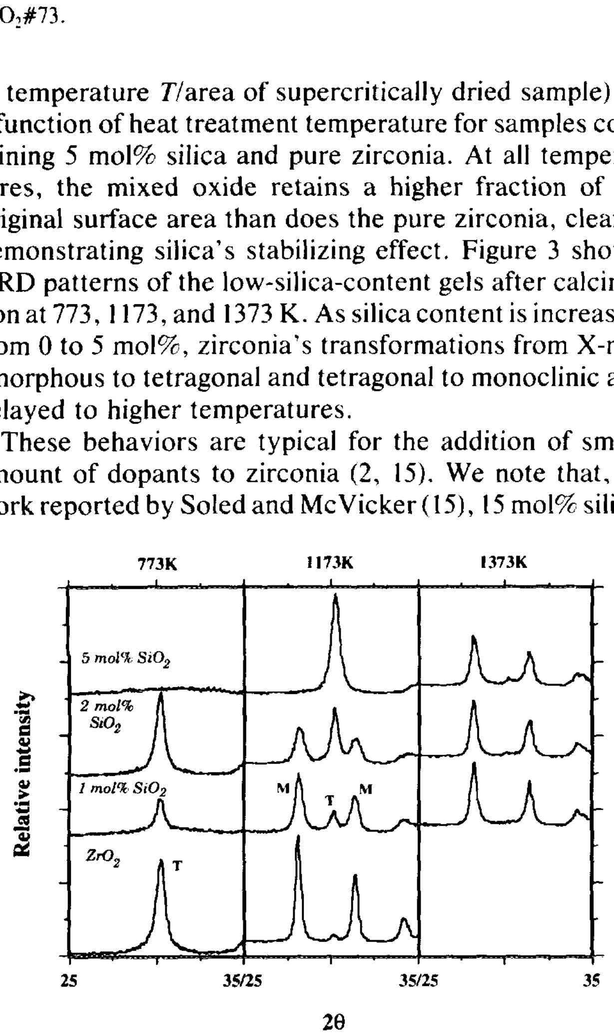

FIG. 3. Effect of calcination temperature on the X-ray diffraction patterns of zirconia–silica aerogels. "T" designates a feature indexed to zirconia's tetragonal phase; "M" is zirconia's monoclinic phase. From bottom to top, the samples are A-$ZrO_2$#73, A-PH-ZS99#3, A-PH-ZS98#2, and A-PH-ZS95#19.

The 95/5 molar ratio of zirconia to silica is important because it represents the lowest silica level capable of stabilizing X-ray amorphous zirconia upon calcination for 2 h at 773 K. We have chosen this composition to examine in detail the effects of homogeneity upon the physical and catalytic properties of zirconia–silica aerogels.

### *The "Stair-Step" Samples—Homogeneity in 95 mol% Zirconia–5 mol% Silica Mixed Oxides*

Our experience with pure zirconia aerogels teaches that textural properties are strong functions of gel time (29). Therefore, to accurately assess the impact of prehydrolysis upon mixed oxide homogeneity, we must decouple its effects from the effects of gel time. We have developed an experimental approach, which we call the stair-step protocol, that allows us to separate the effects of prehydrolysis and gel time. As Fig. 4 shows (note the stair-step shape of the graph), the protocol involves preparation of three pairs of samples. Each pair is made at a constant gel time and each pair has one prehydrolyzed member and one nonprehydrolyzed member. The gel time adjustments are made by varying the total acid content of the synthe-

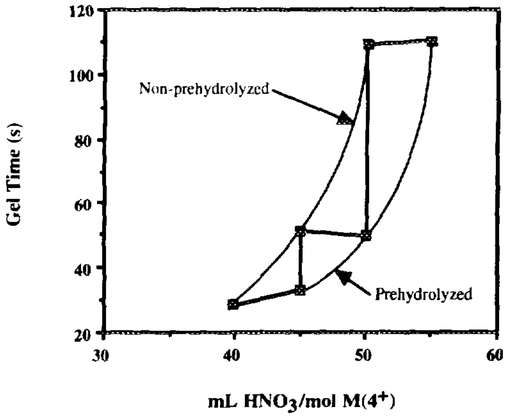

FIG. 4. Schematic diagram of the stair-step synthetic protocol showing the effect of nitric acid content on gel time for both prehydrolyzed and nonprehydrolyzed zirconia–silica mixed oxide gels. Mol $M^{(4+)}$ denotes the total number of moles of zirconium and silicon precursors.

sis—addition of nitric acid causes gel time to increase. One possible explanation of this effect is that by protonating the nucleophilic attacking groups, primarily -OH, the acid makes them less reactive (18). All other synthetic parameters, including precursor concentrations and hydrolysis ratio, are held constant.

Figure 5 displays the variation of BET surface area with gel time for the stair-step samples. Also included in Fig. 5 are data for a 67-s PH gel which we describe in detail later in this paper. For the NPH samples, surface area is not a very strong function of gel time. At low gel times, 50 s and less, the PH gels do not differ significantly from their NPH counterparts. However, at longer gel times, the areas of the PH samples decrease as gel time increases, much like the behavior we have reported for pure zirconia aerogels (29). The pore size distributions of the stair-step gels, which appear in Fig. 6, show similar differences between the PH and NPH preparation techniques. For NPH samples, neither the width of the distribution nor the location of its maximum depends strongly on gel time. The pore distributions of the PH gels, on the other hand, broaden and their centers shift to higher average pore size with increasing gel time. Again, the gel time dependence of the prehydrolyzed gels mirrors the behavior of pure zirconia aerogels (29).

As shown in Fig. 3, pure zirconia aerogel crystallizes into the tetragonal phase upon calcination at 773 K. Figure 7 demonstrates how the presence of 5 mol% silica in the stair-step gels affects zirconia's X-ray amorphous to tetragonal transformation. All samples but one—the 114-s prehydrolyzed gel—are X-ray amorphous or only weakly crystalline after calcination at 773 K for 2 h. The inability of the 114-s PH preparation to prevent crystallization provides additional evidence that, at long gel times, prehydrolyzed zirconia–silica gels behave very much like pure zirconia aerogels.

We have also examined the ~50- and ~115-s members of the stair-step series using DRIFT spectroscopy. Our focus is on a portion of the spectrum near 945 $\mathrm{cm}^{-1}$ that has been assigned to silicon bound to hydroxyl (silanol, Si–OH) (9, 20, 40, 41). Because we expect -OH groups to be located at the surface of the oxide and interior Si atoms to be present in Si–O–Si and Si–O–Zr linkages, the intensity of the silanol signal can be used as a measure

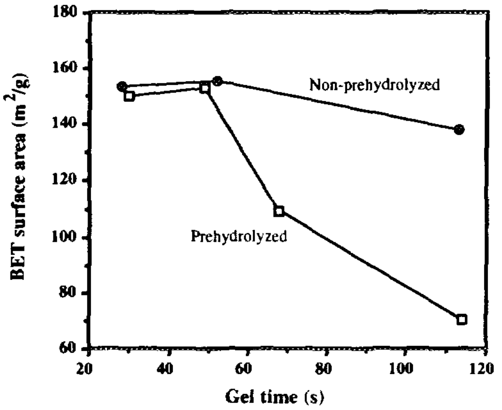

FIG. 5. Effect of gel time on the BET surface area of the stair-step zirconia–silica aerogels. All samples calcined at 773 K in oxygen for 2 h.

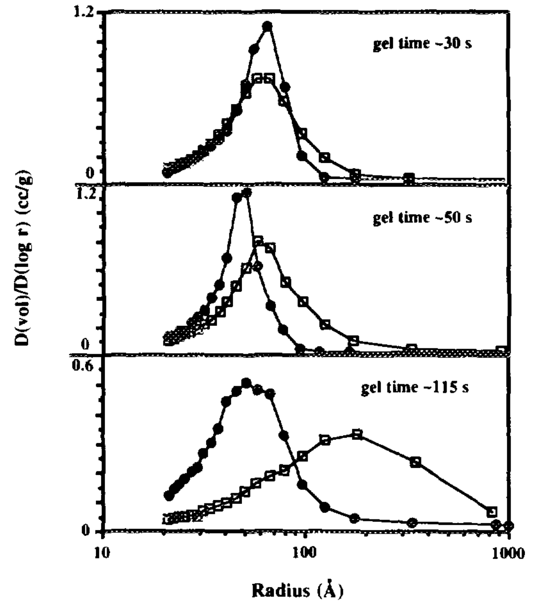

FIG. 6. Effects of prehydrolysis and gel time on the pore size distributions of the stair-step zirconia–silica aerogels. Open symbols, prehydrolyzed samples; closed symbols, nonprehydrolyzed samples. All samples calcined at 773 K in oxygen for 2 h.

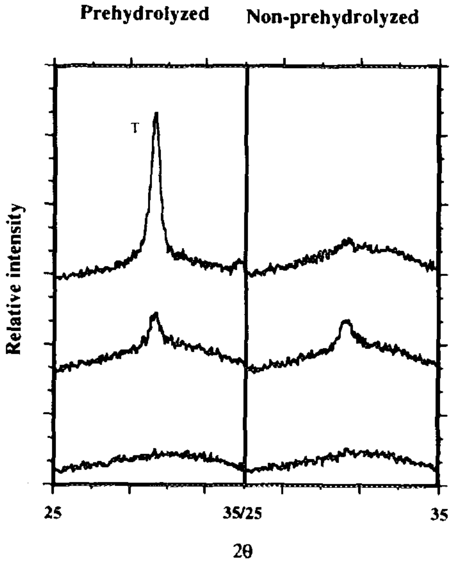

FIG. 7. X-ray diffraction results showing the effect of gel time on the stair-step zirconia–silica aerogels. The peak labeled "T" corresponds to the (111) diffraction of tetragonal zirconia. From bottom to top, gel times are ~30, ~50, and ~115 s. All samples calcined at 773 K in oxygen for 2 h.

of relative *heterogeneity* in these samples—we associate high silanol intensities with segregation of silica at the mixed oxide's surface. As Fig. 8 shows, the silanol intensities of the ~50-s pair and the 113-s NPH sample are comparable. The silanol feature of the 114-s PH sample is less intense, suggesting that it is the most well mixed of this group.

Table 2 presents 1-butene isomerization rates, on a per-surface-area basis, at 5 min on stream using the stair-step mixed oxides as catalysts. All samples except the 114-s PH mixed oxide display low activities, comparable to that of a pure zirconia aerogel. The isomerization rate over the 114-s PH sample is, in contrast, three times higher. Based on Tanabe's work with $TiO_2$–$SiO_2$ and $TiO_2$–ZnO mixed oxides (10), we propose that the high activity of our 114-s PH sample provides additional evidence of its relative homogeneity. Tanabe showed that preparation techniques designed to promote *heterogeneous* mixing tend to produce samples with stronger acid sites—but fewer *total* sites—than do syntheses which promote homogeneous mixing. Furthermore, his homogeneous $TiO_2$–$SiO_2$ samples were more active for 1-butene isomerization than were heterogeneous samples, suggesting that acid site density can be more important than absolute acid strength in this reaction.

The near-unity ratio of *cis*- to *trans*-2-butene products observed in these trials indicates that the isomerization reaction is taking place on Brønsted acid sties (4). Therefore, our activity data demonstrate the effect of preparation on the Brønsted acidity of our samples, not necessarily their total acidity.

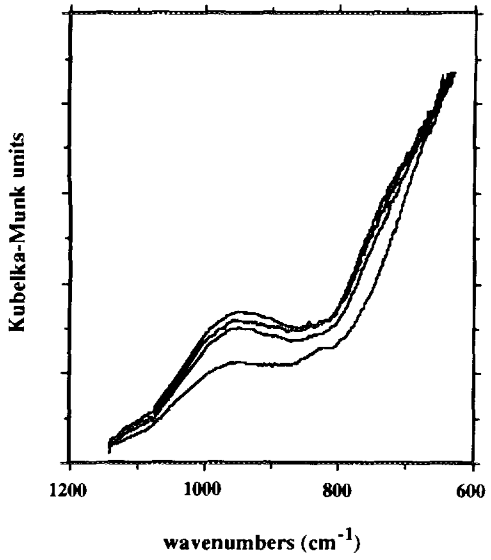

FIG. 8. Si–OH stretching region of the DRIFT spectra of the ~50- and ~115-s pairs of zirconia–silica aerogels. From top to bottom, they are A-NPH-ZS95#25 (113 s NPH), A-PH-ZS95#53 (49 s PH), A-NPH-ZS95#27 (52 s NPH), and A-PH-ZS95#49 (114 s PH). All samples calcined at 773 K in oxygen for 2 h.

TABLE 2

Zirconia–Silica Aerogels: Activity for 1-Butene Isomerization[a]

| Sample | Gel time (s) | Reaction rate (mol × $10^{-3}/m^2/h$)[b] | *cis*/*trans* ratio[b,c] |
|---|---|---|---|
| *Stair-step samples* | | | |
| A-NPH-ZS95#10 | 28 | 0.01 | n/a[d] |
| A-PH-ZS95#53 | 49 | 0.01 | n/a |
| A-NPH-ZS95#27 | 52 | 0.01 | n/a |
| A-PH-ZS95#49 | 114 | 0.03 | 1.60 |
| A-NPH-ZS95#25 | 113 | 0.01 | 1.28 |
| *Alternate reactivity matching techniques* | | | |
| A-PH-ZS95#59 | 67 | 0.04 | 1.06 |
| A-NPH(AC)-ZS95#11 | 64 | 0.07 | 1.27 |
| A-NPH-ZS95#29 | 70 | 0.03 | 1.05 |
| A-NPH(T)-ZS95#3 | 137 | 0.01 | n/a |
| *Other* | | | |
| A-$ZrO_2$#B6 | | 0.01 | n/a |
| A-$SiO_2$[e] | | 0.00 | |
| Blank reactor | | 0.00 | |

[a] All samples calcined in oxygen at 773 K for 2 h.
[b] Measured at 5 min time on stream.
[c] Ratio of *cis*-2-butene to *trans*-2-butene products.
[d] Not available.
[e] See Ref. 46.

We note in passing that the activity displayed by the 114-s PH mixed oxide in 1-butene isomerization, while higher than those of the component single oxides, is low compared to those of samples having higher silica contents. Using the synthetic approach described in this work, we have prepared homogeneous zirconia–silica aerogels with Zr/Si atomic ratios near 1.0. These samples display isomerization rates up to four times as high as that of the 114-s PH stair-step sample. Work in our laboratory to quantify the catalytic performance of high-silica-content gels is in progress.

### *The Effect of Prehydrolysis on the Evolution of Textural Properties*

Based on the evidence presented thus far, we can construct a model of how prehydrolysis affects the evolution of textural properties in the long-gel-time zirconia–silica samples. A schematic diagram of the model appears in Fig. 9. With prehydrolysis, silicon and zirconium precursor reactivities are well matched, allowing silica to be incorporated into the growing zirconia network homogeneously and without disturbing zirconia's normal gelling patterns. The primary particles which first form in the sol are themselves homogeneous, and, as is the case for pure zirconia aerogels, these particles grow with time, accounting for the gel time dependence of textural properties (29).

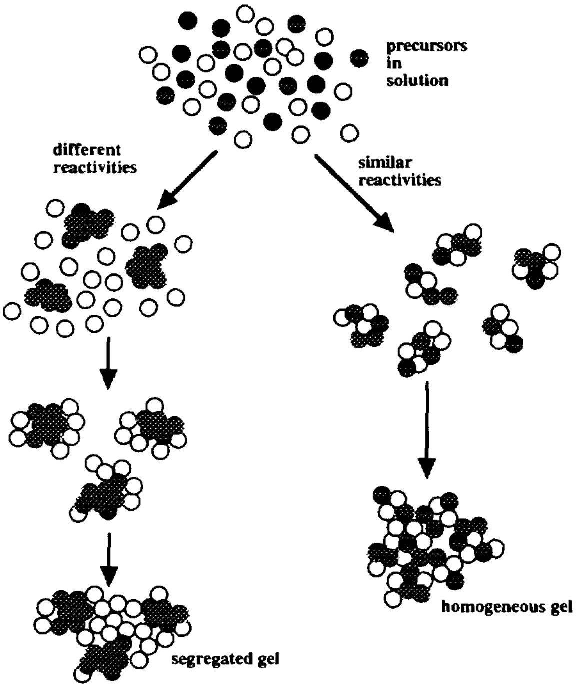

FIG. 9. Schematic diagram of hypothesis regarding differences in textural evolution between prehydrolyzed (right-hand side) and nonprehydrolyzed (left-hand side) zirconia–silica gels.

Finally, when the particles crosslink to form the product alcogel, it too is homogeneous.

In the nonprehydrolyzed case, the first condensation products are likely to be pure zirconia. Since the textural properties of these mixed gels are not functions of gel time, it is possible that the silica precursor recognizes a critical zirconia particle size or extent of reaction at which the zirconia's reduced reactivity matches its own. At this point, the silicon precursor starts to participate in the reactions. When it does, it tends to be located near the surface of the primary particles. When crosslinking occurs at the gel point, the product is a segregated gel.

At low gel times, the characteristics of the PH and NPH gels are essentially the same (see Figs. 5 and 6); both preparation procedures appear to produce heterogeneously mixed oxides. This is probably due to the effect of nitric acid, which we use to control gel time, upon relative precursor reactivity. Nitric acid slows all reactions, but its effect is likely to be most pronounced on reactions involving the more reactive zirconium precursor. Therefore, at long gel times, which we achieve by increasing the acid content of the system, nitric acid works in tandem with prehydrolysis to match precursor reactivities. On the other hand, at short gel times— ~50 s and less—when nitric acid content is low, prehydrolysis itself may not be able to completely match presursor reactivities.

### *Other Strategies for Matching Precursor Reactivity*

We have also matched precursor reactivity in the zirconia–silica system by using a tetramethylorthosilicate precursor in place of tetraethylorthosilicate. In Fig. 10 we compare the textural properties of two gels which demonstrate the effect of the switch. One is a 67-s gel-time prehydrolyzed TEOS gel similar to the PH members of the stair-step series. Since, as shown in Fig. 5, it was prepared with a gel time long enough to allow it to be differentiated from nonprehydrolyzed samples, we expect it to be homogeneously mixed. Also included in Fig. 10 are data for a 70-s gel prepared by using TMOS in the 113-s NPH TEOS formulation. We did not prehydrolyze TMOS because we expect it to be more reactive than TEOS (18, 44, 45). Indeed, TMOS' higher reactivity is confirmed by the decrease in gel time—from 113 to 70 s. Because the two gels in Fig. 10 have similar surface areas at comparable gel times, we conclude that they were prepared by techniques that result in the same *average* relative precursor reactivity. However, the obvious differences between the samples' pore size distributions suggest that there are differences in the details, or quality, of the reactivity match. For example, prehydrolysis may produce a broad distribution of silicon precursor reactivities, while TMOS may display a narrower reactivity range.

We have also arrived at the same gel time/surface area pair by chemically modifying the zirconium precursor. Figure 11 compares the textural properties of the 67-s PH TEOS gel to those of a 64-s acac-modified gel. The acac modification (0.25 mol acac/mol Zr) was applied to the 52-s NPH preparation. As the gel time increase from 52 to 64 s shows, modification of the zirconium precursor did slow the reactions. The time/area match suggests that this gel was prepared with the same average relative pre-

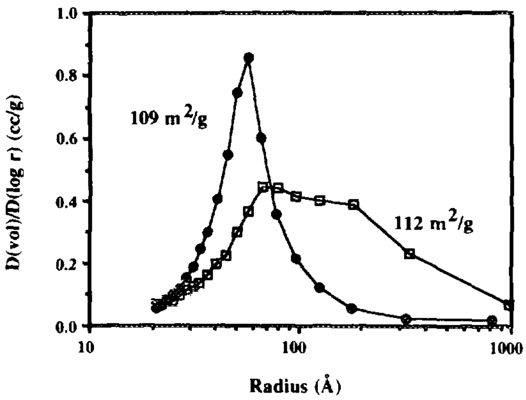

FIG. 10. Precursor reactivity matching by choosing a more reactive precursor molecule: effect on pore size distribution and surface area. Open symbols, 67-s PH gel (A-PH-ZS95#59); closed symbols, 70-s TMOS gel (A-NPH-ZS95#29). Both samples calcined at 773 K in oxygen for 2 h.

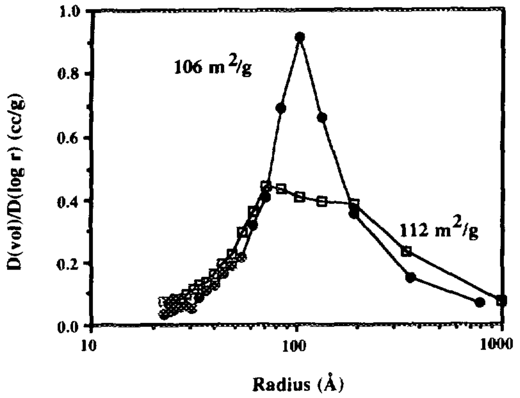

FIG. 11. Precursor reactivity matching by acetylacetone (acac) modification of the zirconium precursor (0.25 mol acac/mol Zr): effect on pore size distribution and surface area. Open symbols, 67-s PH gel (A-PH-ZS95#59); closed symbols, 64-s acac-modified gel A-NPH(AC)-ZS95#11). Both samples calcined at 773 K in oxygen for 2 h.

cursor reactivity as that of the 67-s PH TEOS and 70-s TMOS gels. And again, differences between their pore size distributions may be indicative of differences in the quality of the reactivity match.

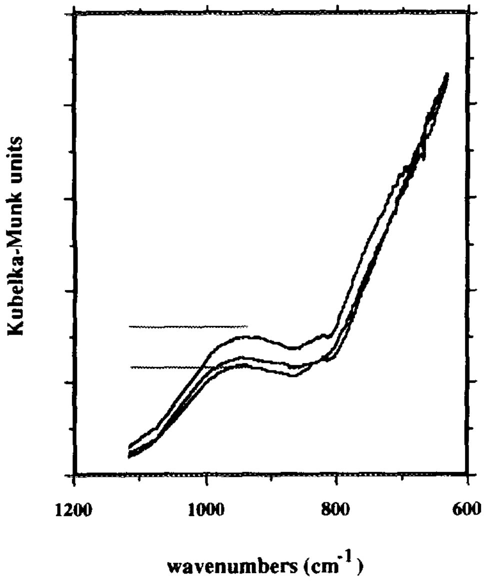

FIG. 12. Si–OH stretching region of the DRIFT spectra of zirconia–silica aerogels prepared by different precursor reactivity matching techniques. From top to bottom, they are A-NPH(AC)-ZS95#11 (acac modified gel), A-PH-ZS95#59 (67-s PH), and A-NPH-ZS95#29 (70-s TMOS). Upper reference line shows peak location for 113-s NPH sample, lower reference for 114-s PH sample (see Fig. 8). All samples calcined at 773 K in oxygen for 2 h.

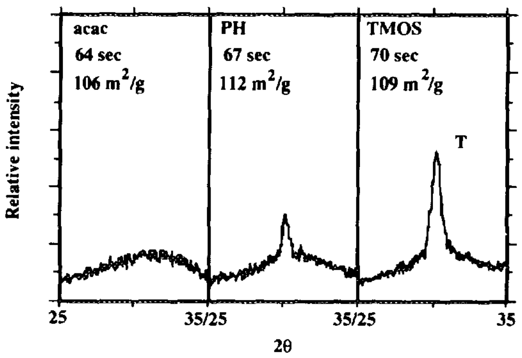

FIG. 13. X-ray diffraction patterns of zirconia–silica aerogels prepared by different precursor reactivity matching techniques. From left to right: A-NPH(AC)-ZS95#11, A-PH-ZS95#59, A-NPH-ZS95#29. All samples calcined at 773 K in oxygen for 2 h.

We have also examined this trio of gels using DRIFT, X-ray diffraction, and 1-butene isomerization. The silanol portions of their IR spectra are shown in Fig. 12, their diffraction patterns in the region indexed to zirconia's tetragonal peak appear in Fig. 13, and their catalytic activities are compared in Table 2. The characteristics of the 67-s PH and TMOS gels are, based on the stair-step evidence, what we would expect of homogeneously mixed oxides: they are at least weakly crystalline, their IR spectra show relatively low silanol intensities comparable to those of the 114-s PH sample, and they are active in 1-butene isomerization.

The acac-modified sample, however, does not fit this pattern. It displays the highest isomerization activity of any 5 mol% silica sample we examined, suggesting that it is homogeneously mixed. On the other hand, its IR and XRD characteristics are more consistent with those of the poorly mixed samples. One plausible explanation is that the surface of the acac sample may be slightly enriched in silica that is, in contrast to the NPH samples, *well dispersed*. Regardless of its dispersion, surface-segregated silica may prevent crystallization of zirconia and give rise to a relatively strong silanol signal in DRIFT. However, perhaps only well-dispersed surface silica—such as we would find in homogeneously mixed samples—is linked to catalytic activity.

Finally, we have adjusted the temperature of the synthesis to try to effect a change in relative precursor reactivity. When we performed the 28-s NPH synthesis in an ice bath, the temperature reduction caused gel time to increase—from 28 to 137 s. However, as shown in Fig. 14, the gel time change is not accompanied by any significant differences in either surface area or pore size distribution, suggesting that relative precursor reactivity has not been affected to any large extent. In fact, since we have previously established the pore size distribution's shift to higher average pore sizes as an indication of well-matched precursor reactivities, the small leftward shift observed in the low-temperature sample could be indicative of further reactivity separation. And, as shown in Table 2, this sample displays low activity for 1-butene isomerization, a characteristic of gels prepared by techniques that do not effectively match precursor reactivities.

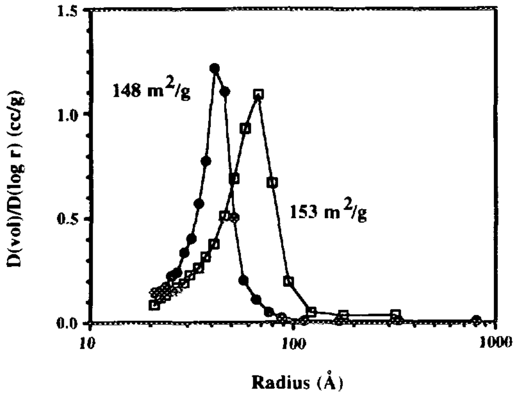

FIG. 14. The effect of synthesis temperature on pore size distribution and surface area of a zirconia–silica aerogel. Open symbols, 28-s NPH gel (A-NPH-ZS95#10); closed symbols, the same synthesis performed in an ice/water bath (A-NPH(T)-ZS95#3). Both samples calcined at 773 K in oxygen for 2 h.

## CONCLUSIONS

We have demonstrated the effectiveness of using sol–gel chemistry, in particular the principle of matching precursor reactivities in two-component systems, to control the physical and catalytic properties of mixed-oxide aerogels. Specifically, we have shown that incorporation of silica, at levels as low as 1–5 mol%, into mixed zirconia–silica aerogels retards the surface area loss and phase transformations that would normally occur in pure zirconia upon heat treatment. At 5 mol% silica, prehydrolysis of the tetraethylorthosilicate precursor can match its reactivity with that of the zirconium precursor. Gels prepared with precursor reactivities matched by prehydrolysis are homogeneously mixed, as demonstrated by (i) the parallel between the gel-time dependence of textural properties in PH mixed oxides and pure zirconia, (ii) the absence of IR evidence for surface-segregated silica, and (iii) activity in 1-butene isomerization. Replacing the TEOS precursor with the more reactive TMOS and chemically modifying the zirconium precursor with acetylacetone are effective alternate strategies for matching precursor reactivities. In addition, the dispersion of surface-segregated silica is an important determinant of isomerization activity.

These results show promising synthetic opportunities to establish a structure–property relationship in mixed oxides. Toward this end, we are extending strategies described in this work to preparation of high-silica-content zirconia–silicas as well as other two-component oxide aerogels.

## ACKNOWLEDGMENT

This work is supported by the Division of Chemical Sciences, Office of Basic Energy Sciences, Office of Energy Research, U. S. Department of Energy (Grant DE-FG02-93ER14345).

## REFERENCES

1. Itoh, M., Hattori, H., and Tanabe, K., *J. Catal.* **35,** 225 (1974).
2. Sohn, J. R., and Jang, H. J., *J. Mol. Catal.* **64,** 349 (1991).
3. Karmakar, B., and Ganguli, D., *Indian J. Technol.* **25,** 282 (1981).
4. Maurer, S. M., and Ko, E. I., *Catal. Lett.* **12,** 231 (1992).
5. Shibata, K., Kiyoura, T., Kitagawa, J., Sumiyoshi, T., and Tanabe, K., *Bull. Chem. Soc., Jpn.* **46,** 2985 (1973).
6. Kijenski, J., and Baiker, A., *Catal. Today* **5,** 1 (1989).
7. Tanabe, K., Sumiyoshi, T., Shibata, K., Kiyoura, T., and Kitagawa, J., *Bull. Chem. Soc. Jpn.* **47**(5), 1064 (1974).
8. Kung, H. H., *J. Solid State Chem.* **52,** 191 (1984).
9. Sohn, J. R., and Jang, H. J., *J. Catal.* **132,** 563 (1991).
10. Tanabe, K., Itoh, M., Morishige, K., and Hattori, H., *in* "Preparation of Catalysts" (B. Delmon, P. A. Jacobs, and G. Poncelet, Eds.), p. 65. Elsevier, Amsterdam, 1976.
11. Tanabe, K., Ishiya, C., Matsuzaki, I., Ichikawa, I., and Hattori, H., *Bull. Chem. Soc. Jpn.* **45,** 47 (1972).
12. Handy, B. E., Baiker, A., Schraml-Marth, M., and Wokaun, A., *J. Catal.* **133,** 1 (1992).
13. Baiker, A., Dollenmeire, P., Glinski, M., and Reller, A., *Appl. Catal.* **35,** 351 (1987).
14. Schraml-Marth, M., Walther, K. L., Wokaun, A., Handy, B. E., and Baiker, A., *J. Non-Cryst. Solids* **143,** 93 (1992).
15. Soled, S., and McVicker, G. B., *Catal. Today* **14,** 189 (1992).
16. Courty, P., and Marcilly, C., *in* "Preparation of Catalysts" (B. Delmon, P. A. Jacobs, and G. Poncelet, Eds.), p. 119. Elsevier, Amsterdam 1976.
17. Ingemar Odenbrand, C., Andersson, S., Andersson, L., Brandin, J., and Busca, G., *J. Catal.* **125,** 541 (1990).
18. Brinker, C., and Scherer, G., "Sol–Gel Science: The Physics and Chemistry of Sol–Gel Processing." Academic Press, Boston, 1990.
19. Campaniello, J., Rabinovich, E., Berthet, P., Revcolevschi, A., and Kopylov, N., *Mater. Res. Soc. Symp. Proc.* **180,** 541 (1990).
20. Nogami, M., *J. Non-Cryst. Solids* **69,** 415 (1985).
21. Nogami, M., and Nagasaka, K., *J. Non-Cryst. Solids* **109,** 79 (1989).
22. Yoldas, B., *J. Non-Cryst. Solids* **38–39,** 81 (1980).
23. Gerardin, C., Sundaresan, S., and Benziger, J., *Chem. Mater.* **6,** 160 (1994).
24. Sanchez, C., Livage, J., Henry, M., and Babonneau, F., *J. Non-Cryst. Solids* **100,** 65 (1988).
25. Papet, P., LeBars, N., Baumard, J., Lecomete, A., and Dauger, A., *J. Mater. Sci.* **24,** 3850 (1989).
26. De, G., Chatterjee, A., and Ganguli, D., *J. Mater. Sci. Lett.* **9,** 845 (1990).
27. Doeff, S., Henry, M., Sanchez, C., and Livage, J., *J. Non-Cryst. Solids* **89,** 206 (1987).
28. Ribot, F., Toledano, P., and Sanchez, C., *Chem. Mater.* **3,** 759 (1991).
29. Ward, D. A., and Ko, E. I., *Chem. Mater.* **5**(7), 956 (1993).
30. Tanabe, K., *Mater. Chem. Phys.* **13,** 347 (1985).
31. Amenomiya, Y., *Appl. Catal.* **30,** 57 (1987).
32. Mizuno, N., Yamato, M., Tanaka, M., and Misono, M., *J. Catal.* **132,** 560 (1991).
33. Iizuka, T., Tanaka, Y., and Tanabe, K., *J. Catal.* **76,** 1 (1982).
34. Hino, M., and Arata, K., *J. Chem. Soc. Chem. Commun.*, 851 (1980).
35. Tanabe, K., and Yamaguchi, T., *in* "Successful Design of Catalysts" (T. Inui, Ed.), p. 99. Elsevier, Amsterdam, 1988.
36. Tseng, S., Jackson, N., and Ekerdt, J., *J. Catal.* **109,** 284 (1988).
37. Pajonk, G., and El Tanany, A., *React. Kinet. Catal. Lett.* **47,** 167 (1992).
38. Kamiya, K., Sakka, S., and Tatemichi, Y., *J. Mater. Sci.* **15,** 1765 (1980).

39. D'yakonov, S., Lygin, V., Shalumov, B., Shepalin, K., Kuznetsnov, A., Kostina, V., and Rastorguev, Y., *Izv. Akad. Nauk. SSSR Neorg. Mater.* **20**(1), 97 (1984).
40. Miranda Salvado, I., Serna, C., Fernandez Navarro, J., *J. Non-Cryst. Solids* **100,** 330 (1988).
41. Lee, S., and Condrate, R., *J. Mater. Sci.* **23**(8), 2951 (1988).
42. Marquez-Alvarez, C., Fierro, J., Guerrero-Ruiz, A., and Rodriuiguez-Ramos, I., *J. Colloid Interface Sci.* **159,** 454 (1993).
43. Maurer, S. M., Ng, D., and Ko, E. I., *Catal. Today* **16,** 319 (1993).
44. Artaki, I., Sinha, S., and Jonas, J., *Mater. Lett.* **2**(5B), 448 (1984).
45. Assink, R. A., and Kay, B. D., *Colloids Surf. A* **74,** 1 (1993).
46. Maurer, S. M., Ph.D. thesis, Carnegie Mellon University, 1991.